Impact of clip connection and insulation thickness on bracing of purlins in standing seam roof systems

Michael W. Seek[1], Daniel McLaughlin[2]

Abstract

The flexural strength of purlins in standing seam roof systems is highly dependent upon the extent to which the sheathing provides lateral and torsional restraint. Typical models to predict the restraint provided by the sheathing assume that the plane of lateral resistance occurs at the top flange of the purlin. In reality, depending on the configuration of the clip and the amount of insulation located between the purlin and the clip, the plane of lateral resistance and corresponding center of rotation shifts above the top flange. This distance, referred to as the effective standoff, is important to evaluate the effectiveness of the sheathing to brace the purlin. A series of 25 tests is performed on a variety of clip, panel, seam and insulation configurations to determine both the effective standoff and rotational stiffness of the panel-clip connections. Test results are reported and recommendations are provided to estimate the effective standoff for use in models to evaluate the effectiveness of the sheathing to brace the purlin. The implications of the effective standoff in the evaluation of purlin bracing are discussed through a parametric comparison of standing seam systems.

1. Background

Standing seam roof systems supported by cold-formed C- and Z-section purlins are gaining popularity because of the durability, efficiency, environmental performance and sustainability of these systems. The purlins in these are typically spaced at 3 to 5 foot intervals and span 20 to 35 feet between primary framing. Insulation is draped over the purlins and a metal clip is fastened through the insulation into the top flange of the purlin with self-tapping screws. The standing seam sheathing is then attached to the clip via a tab on the clip that interlocks into the seam of the panel. The seam of each panel interlocks with the adjacent panel and is often mechanically crimped. By enclosing the connection to the clip within the seam, penetrations through the sheathing and, thus, potential avenues for leaks, are minimized.

There are two main types of panel profiles: vertical rib and trapezoidal. Vertical rib profiles have a slender vertical rib and typically have widths between seams of 12 in. to 16 in. Trapezoidal panels, as the name implies, are profiled into a trapezoidal shape that increases the stiffness of the seam allowing for longer spans. Trapezoidal profiles are typically 24 in. wide. Each profile

---

[1] Assistant Professor, Old Dominion University, <mseek@odu.edu>
[2] Undergraduate Research Assistant, Old Dominion University, <dmcla013@odu.edu>

utilizes clips specific to the rib profile. Clips may also be provided in two different heights (either *low* or *high*) to account for differing insulation thicknesses. Low clips are used with insulation thickness ranging from 0" to 4" whereas high clips are used with insulation ranging from 2" to 6". Because these systems are often used to cover large areas, flexibility is often designed into the clip connection to allow for thermal expansion/contraction. Clips with built-in flexibility are referred to as *sliding* whereas those without are referred to as *fixed*. Designs for sliding clips can vary widely, however, in surveying the different clips available within the industry, a sub-category of sliding clips was created. Sliding clips were subcategorized as: *sliding tab*, where the main body of the clip has a rigid structure with a sliding tab that fits into the seam (Fig 1(a)), or *floating*, where the clip has a base that is attached to the purlin and the main body of the clip fits into the seam and slides as a unit (Fig. 1(b)).

(a) High clip - Sliding tab   (b) High Clip – Floating
Figure 1: Sliding trapezoidal clip profiles

Cold-formed C- and Z-section purlins in standing seam roof systems rely on the lateral and torsional restraint provided by the sheathing for strength and stability. C-sections, because of the eccentricity of the shear center are subject to torsion along the length which is partially restrained by the sheathing. In addition to torsion, Z-sections, as a result of the inclined principal axes, are also subject to lateral deflections that are resisted by the sheathing. The restraint provided by the sheathing to the purlin is translated into in-plane diaphragm forces in the sheathing that is extracted from the system through *anchors*.

The Component Stiffness Method (Murray et al. 2009) was developed to quantify the anchorage forces that must be extracted from the diaphragm. Further research into the method showed that the method can be expanded to determine the changes in stresses in the purlin cross section as flexibility is introduced in the system (Seek and Escobales, 2015). Whereas these systems have typically been analyzed with the assumption of a constrained stress distribution, Seek et al (2016) showed that the changes in stress profile can significantly impact the predicted local and distortional buckling strength and allows for better alignment with test results. Thus, the method provides powerful insight into the behavior of purlin-sheathing systems.

The method uses a displacement compatibility approach to define the extent to which the sheathing restrains the purlin. The sheathing provides restraint through a torsional spring at the top flange representing the rotational stiffness of the connection between the panel and the purlin and a lateral spring representing the diaphragm stiffness of the sheathing. In the original formulation of this method, displacement compatibility was enforced at the top flange of the purlin. In reality, because the connection between the purlin and sheathing is separated by insulation and a clip that is the height of the standing seam rib, the point of displacement compatibility is offset from the top flange relative to the height of the clip (Fig. 2). Quantifying this distance, referred to as the effective standoff, is the goal of this research.
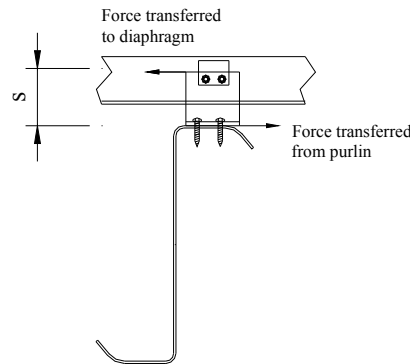

Figure 2: Lateral force transfer through clip

2. Test to Determine Effective Standoff

For the sheathing to laterally restrain the purlin, horizontal forces generated in the purlin must be transferred over the height of the clip to the sheathing, creating a moment in the connection. The clip itself is treated as a rigid body but the purlin-clip connection and the clip-sheathing connection both have flexibility and may be modeled as springs. If the purlin-clip connection is flexible relative to the clip-sheathing connection, the clip will act rigidly with the sheathing and the standoff will be minimized as shown in Fig. 3(a). Conversely, if the clip-sheathing connection is flexible relative to the clip-purlin connection, the standoff distance will equal the clip height as shown in Fig. 3(b). In reality, as the flexibility of the sheathing-clip connection increases relative to the purlin clip connection, the standoff increases. The standoff therefore has a range between zero and the height of the clip (measured to the shoulder of the clip where it contacts the bottom of the sheathing) as shown in Fig 3(c).

(a) standoff = 0 in.   (b) standoff = clip height   (c) 0 < standoff < clip height
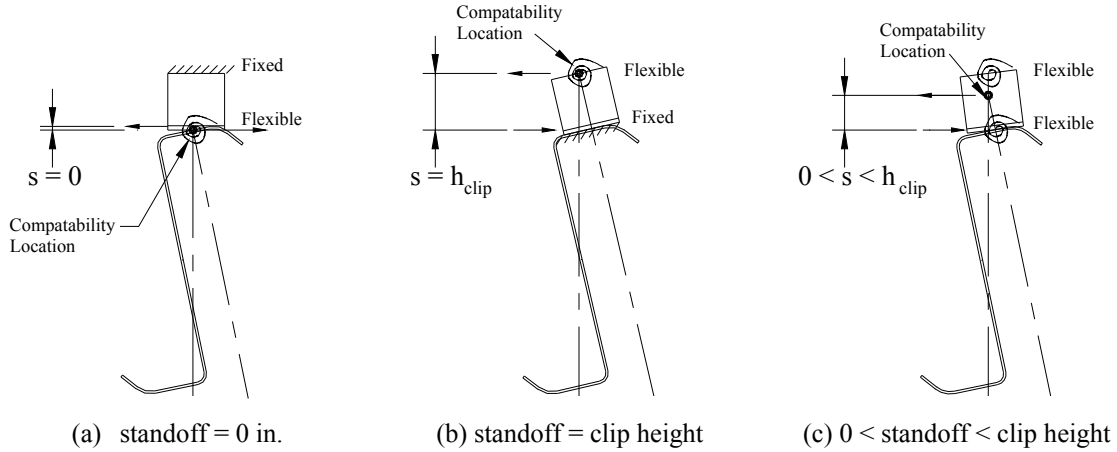
Figure 3: Standoff Range

The AISI test standard S901-13 *Rotational-Lateral Stiffness Test Method for Beam-to-Panel Assemblies* (AISI 2013) outlines the test apparatus and procedure to determine the rotational stiffness of the connection between the purlin and sheathing. In the test, a force is applied to the free flange of the purlin parallel to the rib of the sheathing as shown in Fig. 5. The displacement of the free flange is measured and the rotational stiffness is determined as the moment resisted per unit rotation. To determine the effective standoff, additional displacement measurements are required. As shown in Fig. 4, to determine the total rotation of the purlin, lateral displacements are measured at the free flange, Δ_1, and the attached flange Δ_2. To measure the relative rotation between the clip and purlin, displacement transducers were attached to the web of the purlin and measured the relative displacement at each end of the clip, Δ_3 and Δ_4. The total rotation of the purlin relative to its original orientation, ϕ_{total}, the rotation of the purlin relative to the clip ϕ_{purlin}, and the rotation of the clip relative to the sheathing, ϕ_{clip}, are shown in Fig. 4 and are calculated:

$$\phi_{total} = a\sin\left(\frac{\Delta_1 - \Delta_2}{d}\right) \tag{1}$$

$$\phi_{purlin} = a\sin\left(\frac{\Delta_4 - \Delta_3}{b_{sensor}}\right) \tag{2}$$

$$\phi_{clip} = \phi_{total} - \phi_{purlin} \tag{3}$$

The unit rotational stiffness of the connection, k_ϕ is calculated

$$k_\phi = \frac{P \cdot h}{\phi_{total} \cdot L_{trib}} \tag{4}$$

where L_{trib} is the length along the purlin tributary to each clip (equal to the clip spacing). The rotational stiffness of both the purlin and the clip can be similarly calculated by comparing the moment to the rotation of the clip or purlin individually.

The effective standoff is defined from the ratio of the clip rotation to the total rotation

$$s = h_{clip} \frac{\phi_{clip}}{\phi_{total}} \tag{5}$$

The height of the clip, h_{clip}, is defined differently between vertical rib profiles and trapezoidal profiles. For vertical rib profiles the height of the clip is the distance from the base of the clip the top edge of the clip that is enclosed in the seam. For trapezoidal profiles, the height of the clip is the distance from the base of the clip to the "shoulder" of the clip that fits under the seam.

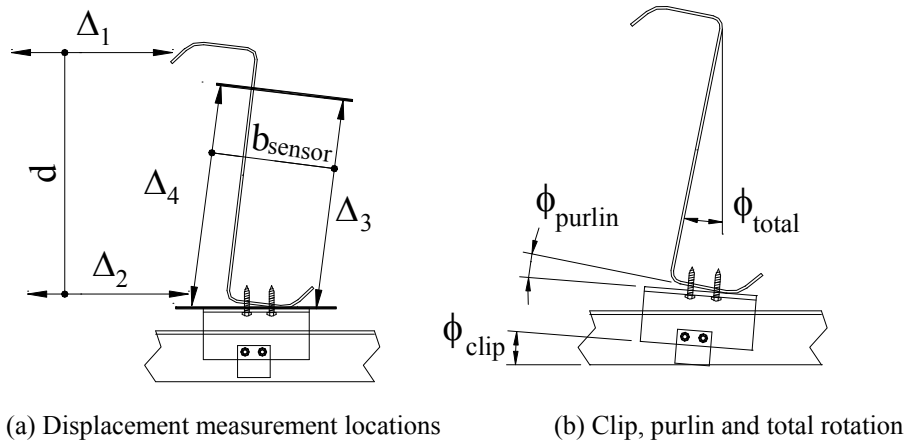(a) Displacement measurement locations   (b) Clip, purlin and total rotation
Figure 4: Quantifying rotational deformation

2.1 Test Program
A survey of clips used by members of the Metal Building Manufacturers Association (MBMA) was undertaken to compare and categorize the clips. From the survey of clips, a test program was developed to investigate and compare the categorized systems. The twenty test configurations (shown in Table 1) chosen provided enough variety to encompass the wide spectrum of systems while still allowing for comparison between systems. Five additional tests were performed to investigate the impact of an un-crimped seam (indicated in the table with a "U" designation).

Table 1: List of Configurations Tested

Trapezoidal Profile			Vertical Rib Profile		
Test #	Clip	Insulation	Test #	Clip	Insulation
1	Low Fixed	0"	13	Low Fixed	0"
2 / 2U[1]		4"	14		4"
3 / 3U[1]	High Fixed	4"	15 / 15U[1]	High Fixed	4"
4		6"	16		6"
5	Low Sliding Tab	0"	17	Low Floating	0"
6		4"	18		4"
7	High Sliding Tab	4"	19	High Floating	4"
8		6"	20		6"
9	Low Floating	0"			
10 / 10U[1]		4"			
11 / 11U[1]	High Floating	4"			
12		6"			

[1]Seam un-crimped

The tests were performed with two panel sections, a tributary purlin section, and a single clip with a strip of insulation 6" wide along the length of the purlin. The purlin cross section in each

test is 8ZS300x0.100. A heavy gauge purlin was chosen to minimize the purlin deformation and virtually no deformation of the purlin was observed. The width of the trapezoidal panel was 24 in. and the vertical rib panel was 16 in. The length of the purlin section used for the trapezoidal test was 24 in. and was 16 in. for the vertical rib test.

The specimen was tested in a simple span configuration shown in Fig 5. The panels are fastened at each end to the test frame with the end nearest the applied load free to rotate and the far end free to translate and rotate (simulating a pin/roller configuration). No fasteners were applied along the edges of the panel to allow the panel to bend along its span although very little deformation of the panel was observed. Two small steel strips spanned across the seam on each side of the purlin and were fastened through the panel to simulate the restraint of adjacent panels and prevent the seam from prematurely opening. The seams were crimped with a single stage hand crimper except in the five un-crimped tests where the seams were simply snapped into place.
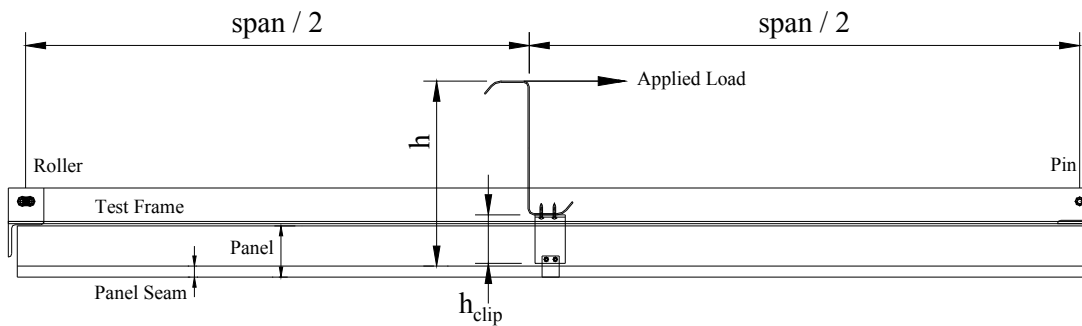

Figure 5: Rotational-lateral stiffness test configuration

The specimen was instrumented to capture the displacements as shown in Fig. 4. Axial force was applied through a threaded rod tightened against an anchor point and was measured with a 2000 lb. S-type load cell and displacements were measured with a mix of wire potentiometers and dial gauges.

2.2 Test Results
Fig. 6 displays the raw test data of the typical behavior of the lateral deflection of the free flange relative to the applied moment. Initially the system exhibits linear behavior but then softens as the compression edge of the clip pries apart the seam. Once the compression edge of the clip fully penetrates the seam, the system continues to deform with little additional applied force. There are also several small dips in the plot. Throughout the test, the loading was paused and at each pause, a slight relaxation of the system was observed.
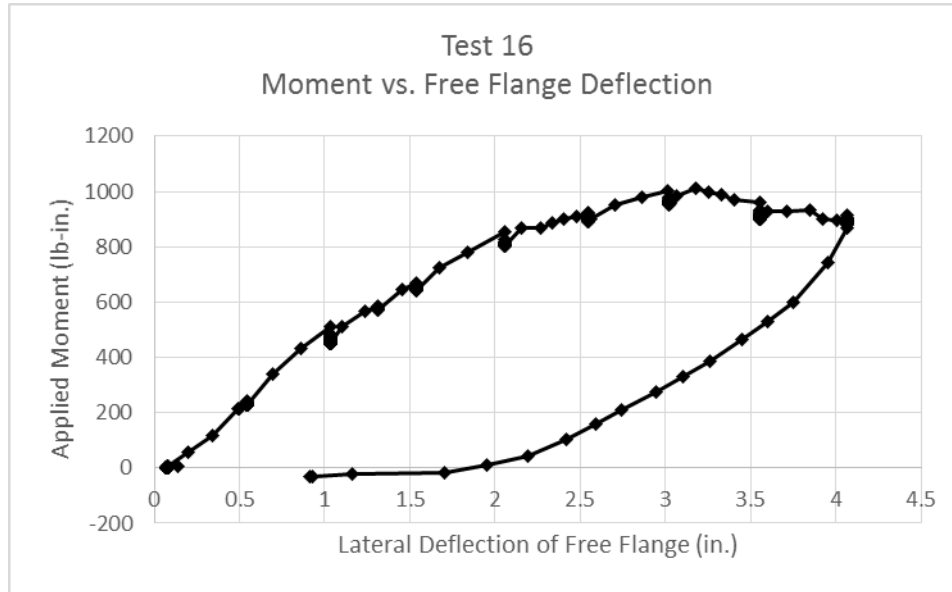
6

Figure 6: Test 16 Moment vs Free Flange Deflection

Fig. 7 shows the clip rotation, the purlin rotation, and total rotation relative to the applied moment. As expected, the purlin rotation relative to the applied moment is constant and thus the stiffness is linear. The non-linearity arises from the clip rotation relative to the deck when, as discussed above, the compression edge of the clip begins to plow into the seam. The total rotation is the combined rotation of the purlin and clip.

The calculated standoff and stiffness are shown in Table 2 and Table 3 for trapezoidal and vertical rib profiles respectively. The measured clip height is the height from the base of the clip to the "shoulders" that fit underneath the seam for a trapezoidal deck. For vertical rib profiles, the measured clip height it the distance from the base of the clip to the top where it fits in the seam. The total height of the clip includes the insulation thickness. When sandwiched between the clip and the purlin, the insulation significantly compresses. The 4 in. insulation reduces to a thickness of 3/32 in. and the 6 in. insulation reduces to 1/8 in.

For a given configuration, as additional thickness of insulation is added between the clip and purlin, the total rotational stiffness decreases as expected. However counter to initial expectations, the additional thickness of insulation actually reduces the effective standoff. The added insulation reduces the stiffness of the connection between the purlin and the clip, thereby increasing the purlin rotation relative to the clip rotation and thus shifting the standoff lower. In general, the effective standoff lies between 50% and 60% of the clip height for the trapezoidal systems tested with a few outlier results. The effective standoff is slightly lower for the vertical rib systems tested, typically falling between 40% and 50% of the clip height again with a few outlier results.

Table 4 compares the results of the five systems that were tested with un-crimped seams with their crimped counterparts. In all cases as expected, the un-crimped seam reduces the stiffness of the clip-sheathing connection and thus the overall stiffness. This decrease in stiffness of the clip-sheathing connection corresponds with an increase in the standoff height. With the un-crimped or snap seam, the standoff distance ranged between 80% and 90% of the clip height.
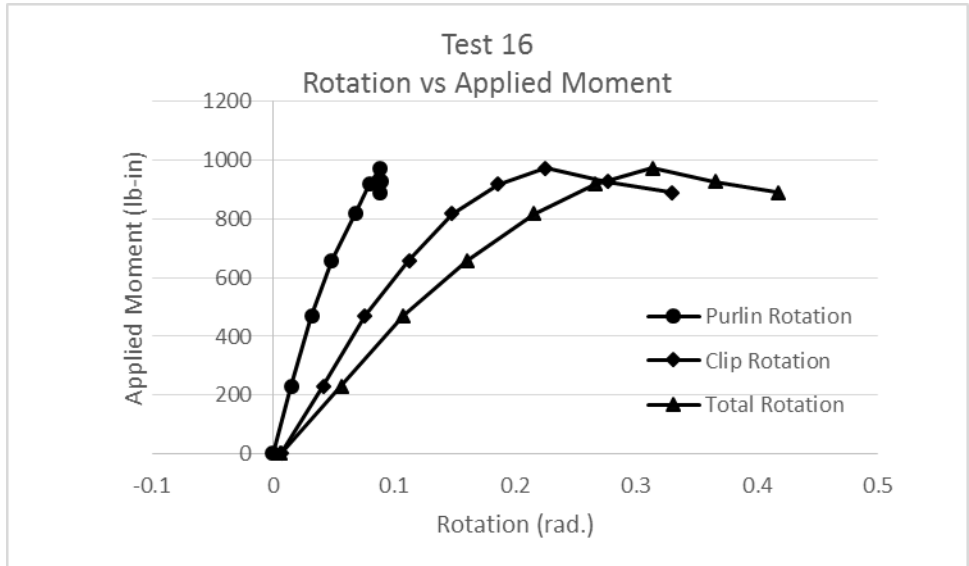
Figure 7: Test 16 Rotation vs. Applied Moment

Table 2: Trapezoidal Rib Standoff and Stiffness Results

Test	Clip Height (in.)	Total Height (in.)	Standoff (in.)	Total Stiffness (lb-in./rad)	Unit Stiffness (kip-in./in./rad)
1	3.5	3.50	2.1	2880	0.120
2	3.5	3.59	2.69	2690	0.112
3	4.5	4.59	3.02	2800	0.117
4	4.5	4.63	2.28	2140	0.089
5	3.375	3.38	3.07	3200	0.133
6	3.375	3.47	2.66	3490	0.146
7	4.375	4.47	2.86	4690	0.195
8	4.375	4.50	2.27	3320	0.138
9	3.5	3.50	2.25	5650	0.235
10	3.5	3.59	2.09	6400	0.267
11	4.5	4.59	2.43	5950	0.248
12	4.5	4.63	2.23	5650	0.235

Table 3 Vertical Rib Standoff and Stiffness Results

Test	Clip Height (in.)	Total Height (in.)	Standoff (in.)	Total Stiffness (lb-in./rad)	Unit Stiffness (kip-in./in./rad)
13	2.375	2.38	1.16	3700	0.231
14	2.375	2.47	1.14	3680	0.230
15	3	3.09	1.59	3440	0.215
16	3	3.13	1.56	3180	0.199
17	2.5	2.50	1.16	5870	0.367
18	2.5	2.59	0.91	4270	0.267
19	3	3.09	0.43	2350	0.147
20	3	3.13	0.42	2170	0.136

Table 4 Crimped vs Un-crimped Standoff and Stiffness Results

Test	Clip Height (in.)	Total Height (in.)	Standoff (in.)	Total Stiffness (lb-in./rad)	Unit Stiffness (kip-in./in./rad)
2	3.5	3.59	2.69	2690	0.112
2U	3.5	3.59	3.28	1920	0.080
3	4.5	4.59	3.02	2800	0.117
3U	4.5	4.59	3.86	1210	0.051
10	3.5	3.59	2.09	6400	0.267
10U	3.5	3.59	2.61	3510	0.146
11	4.5	4.59	2.43	5950	0.248
11U	4.5	4.59	3.77	3860	0.161
15	3	3.09	1.59	3440	0.215
15U	3	3.09	2.74	1050	0.066

3. Impact of standoff on anchorage forces

To investigate the impact of changes in standoff distance on anchorage forces in purlin supported roof systems, the anchorage forces are calculated for a suite of nineteen purlin cross sections. The cross sections are a representative sample of the purlins in use with depths ranging from 6 in. to 12 in., flange widths ranging from 2.25 in. to 3.25 in., and thicknesses from 0.059 in. to 0.105 in. The effect of changes in diaphragm stiffness and the rotational stiffness of the connection were investigated as well. The diaphragm stiffness, G', ranged from stiff (1000 lb/in) to flexible (100 lb/in) and the total rotational stiffness of the connection ranged from 0.250 kip-in./in./rad. to 0.100 kip-in./in./rad. Data points were taken at 3 different roof pitches: 0:12, 3:12, 6:12. The results of this comparison are shown in Fig. 8.

In Fig. 8, the cluster of data in the upper right represents the anchorage force at low slope (0:12) while the lower right represents the anchorage force at high slope (6:12). The diagonal line represents a 1:1 correlation. At the low slope, as the standoff is increased the anchorage force increases. The changes are most drastic for the shallowest purlins, primarily because the change in standoff is much larger in proportion to the depth of the purlin. As the roof slope increases, the anchorage forces shift direction (a negative anchorage force prevents a downslope translation). The magnitude of the anchorage forces again increase as the standoff distance is increased. Given this behavior, a conservative estimate of the standoff distance will result in a conservative approximation of the anchorage forces.

Fig. 9 plots the simple span supports restraint anchorage force vs roof slope for a single purlin (8ZS2.25x070) for four different combinations of standoff eccentricity and eccentricity of applied load on the top flange of the purlin. The eccentricity of the applied load on the top flange is usually reported as a proportion of the flange width, δ. In Fig. 9, as the top flange eccentricity, δ, increases, the y-intercept of the trend line increases. As the standoff eccentricity increases, the y-intercept increases coupled with an increase in the magnitude of the slope. In previous models aimed at predicting the anchorage force in purlin roof systems, there has been some uncertainty in the eccentricity of the applied load, typically predicted between one-sixth and one-half the width of the flange. In these prediction models, standoff eccentricity has not been considered. By including standoff eccentricity in these prediction models, it is likely that these discrepancies in the top flange eccentricity can be eliminated.
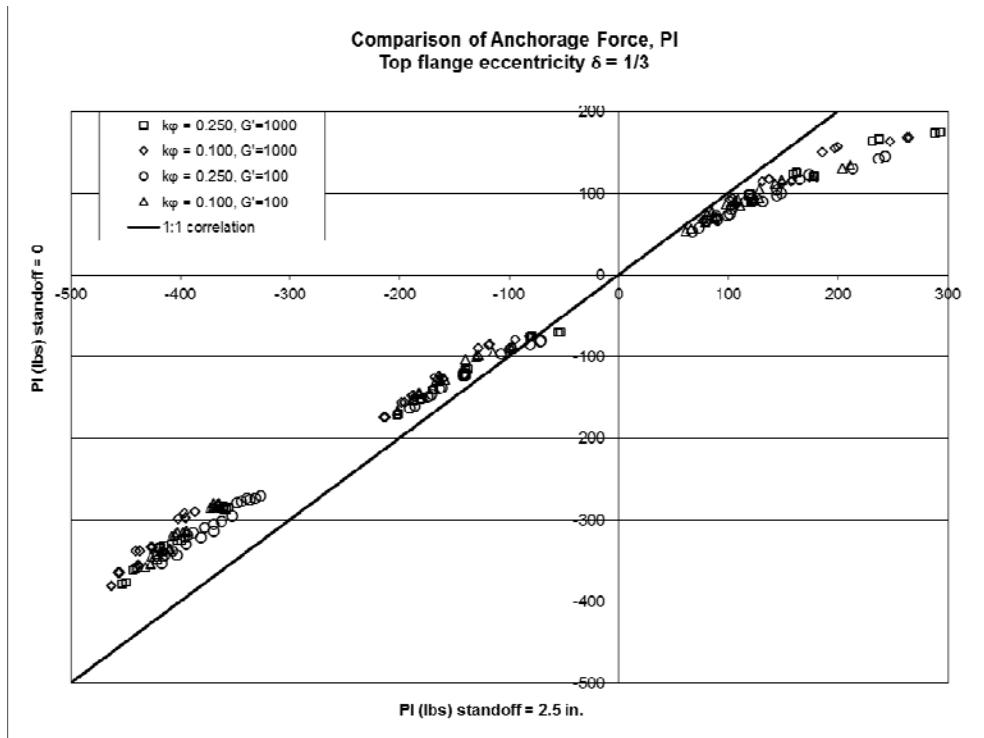
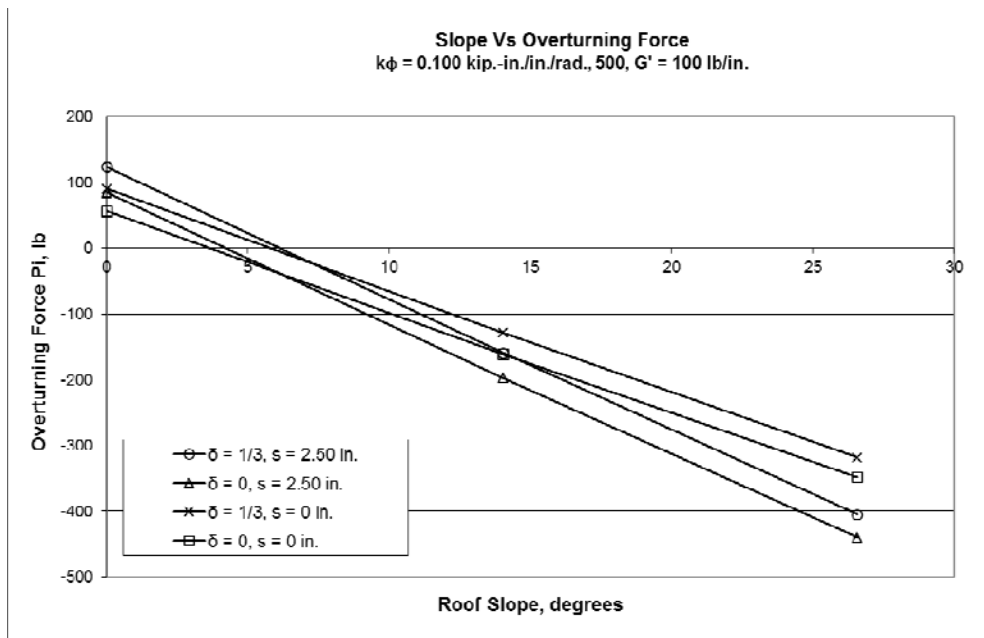Figure 8: Impact of standoff distance on anchorage force

Figure 9: Comparison of load eccentricity and standoff eccentricity for flexible system

4. Conclusions

The effective standoff distance created by the separation between the purlin and sheathing is an important consideration in the design of purlin supported standing seam roof systems. This standoff distance impacts the moment-rotation behavior of the purlin which in turn impacts the anchorage forces in purlin roof systems. Adding layers of insulation between the standing seam clip and purlin will reduce the rotational stiffness of the connection as well as lower the effective

standoff distance. The effective standoff can easily be determined by collecting additional displacement data from the existing AISI S901-13 Rotational-Lateral Test Method. In lieu of test data, the effective standoff can be approximated as 60% of the clip height for crimped trapezoidal profiles, 50% of the clip height for crimped vertical rib profiles, and 90% of the clip height for un-crimped trapezoidal and vertical rib profiles. Further research is needed to evaluate the interaction between the standoff distance and eccentricity of the applied load in the determination of anchorage forces. Further research is also required to investigate the impacts of the increase in standoff on the flexural strength of purlin roof systems.

Acknowledgments

References

AISI (American Iron and Steel Institute). (2013) S901-13 *Rotational-Lateral Stiffness Test Method for Beam-to-Panel Assemblies*. Washington, DC.

AISI (American Iron and Steel Institute). (2012). North American Specification for the Design of Cold-Formed Steel Structural Members. Washington, DC.

Murray, T. M., Sears, J., and Seek, M. W. (2009). *D111-09 Design Guide for Cold-Formed Steel Purlin Roof Framing Systems*. American Iron and Steel Institute. Washington, DC.

Seek, M**.** and Escobales, N. (2015). "Computational Procedure for Normal Stresses in C-Sections and Z-Sections with One Flange Attached to Sheathing." *J. Struct. Eng.* , 10.1061/(ASCE)ST.1943-541X.0001412 , 04015143.

Seek, M. W. (2016) ''A Combined Direct Analysis and Direct Strength Approach to Predict the Flexural Strength of of Z-Purlins with Paired Torsion Braces.'' *23rd International Specialty Conference on Cold-Formed Steel Structures.* November 10, 2016. Department of Civil Engineering, University of Missouri-Rolla, Rolla, Missouri.